

# Probing 3D Collective Cancer Invasion Using Double-Stranded Locked Nucleic Acid Biosensors

Zachary S. Dean,<sup>†</sup> Paul Elias,<sup>†</sup> Nima Jamilpour,<sup>‡</sup> Urs Utzinger,<sup>†</sup> and Pak Kin Wong<sup>\*,†,‡,§</sup>

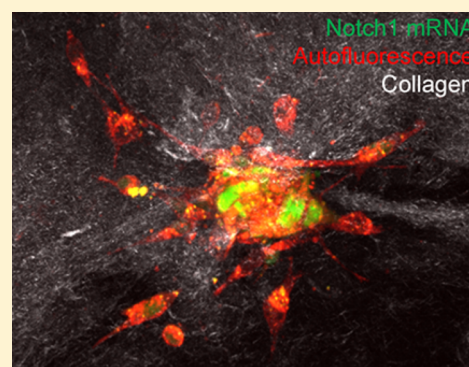
<sup>†</sup>Department of Biomedical Engineering, The University of Arizona, Tucson, Arizona 85721, United States

<sup>‡</sup>Department of Aerospace and Mechanical Engineering, The University of Arizona, Tucson, Arizona 85721, United States

<sup>§</sup>Department of Biomedical Engineering, Mechanical Engineering and Surgery, The Pennsylvania State University, University Park, Pennsylvania 16802, United States

## Supporting Information

**ABSTRACT:** Cancer is a leading cause of death worldwide and metastases are responsible for over 90% of human cancer deaths. There is an urgent need to develop novel therapeutics for suppressing cancer invasion, the initial step of metastasis. Nevertheless, the regulation of cancer invasion is poorly understood due to a paucity of tools for monitoring the invasion process in 3D microenvironments. Here, we report a double-stranded locked nucleic acid (dsLNA) biosensor for investigating 3D collective cancer invasion. By incorporating multiphoton microscopy and the dsLNA biosensor, we perform dynamic single cell gene expression analysis while simultaneously characterizing the biomechanical interaction between the invading sprouts and the extracellular matrix. Gene profiling of invasive leader cells and detached cells suggest distinctive signaling mechanisms involved in collective and individual invasion in the 3D microenvironment. Our results underscore the involvement of Notch signaling in 3D collective cancer invasion, which warrants further investigation toward antimetastasis therapy in the future.



Tumors often invade as adherent groups of cells with invasive leader cells at the invading fronts guiding collective cancer invasion.<sup>1–3</sup> For instance, squamous cell carcinomas invading in the form of clusters or strands were reported in histopathological and venous outflow analyses.<sup>4–6</sup> In a breast tumor organoid model, invasive leader cells were observed to lead the invasion of cohesive multicellular units.<sup>3</sup> Collective invasion and the dynamic exchange of leader cells in the invading front were observed for metastatic cancer cells in a 3D collagen matrix.<sup>7</sup> In an organotypic coculture invasion model, carcinoma-associated fibroblasts were demonstrated to serve as leaders and drive collective cancer invasion of carcinoma cells.<sup>8,9</sup> Interestingly, biophysical factors, such as mechanical compression, cell traction force, and intercellular tension,<sup>10–12</sup> were shown to modulate leader cells, suggesting a mechanistic linkage between the biophysical microenvironment and collective cancer invasion.

While many studies have investigated cancer cell migration in 2D, examining the spatiotemporal dynamics of 3D collective cancer invasion is inherently difficult due to the complex cell-matrix interactions and additional imaging dimension. In order to solve this problem, we have developed a double-stranded locked nucleic acid (dsLNA) biosensor that allows for dynamic single-cell gene expression analysis in living cells.<sup>13–16</sup> The biosensor features a 5'-conjugated donor fluorophore in addition to an adjacent 3'-conjugated Dark Quencher, Iowa Black FQ. When a target RNA (e.g., mRNA or miRNA) is

present, the donor and the quencher strands separate, the quencher moves away from the donor, and fluorescence is detected. Using this biosensor, we have previously demonstrated that real-time RNA expression can be monitored in living cells during 2D migration.

Herein, we adapt dsLNA probes for investigating leader-follower organization during 3D collective cancer invasion (Figure 1). We explore key signaling pathways involved in 3D cancer invasion, findings that may have implications in the development of novel targets for antimetastasis therapy. Notch-1 and Dll4, for instance, have both been implicated in angiogenesis and tumorigenesis, and in addition, have shown importance in leader cell formation in 2D cell migration.<sup>11,17–19</sup> However, the influence of Notch signaling remains unclear during collective cancer invasion in 3D microenvironments. We therefore incorporate dsLNA probes for dynamic gene expression profiling in invading 3D cancer spheroids. Multiphoton microscopy is included to monitor 3D collective cancer invasion, characterize collagen I remodeling via second harmonic generation, and increase the imaging depth and signal-to-noise ratio over traditional microscopes. The dsLNA probe allows for not only measurements of invasive leader cells

Received: July 10, 2016

Accepted: August 9, 2016

Published: August 16, 2016

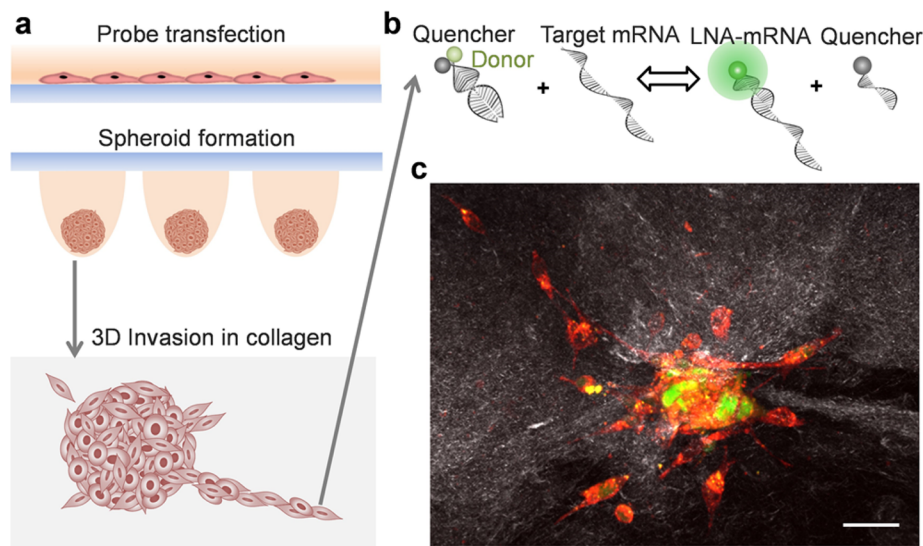


**Figure 1.** Dynamic single-cell gene expression analysis of invading cancer cells in 3D microenvironments. (a) Schematic of the 3D spheroid invasion assay. The dsDNA probes are first transfected into MDA-MB-231 cells before spheroid formation with the hanging drop method. The spheroids are then resuspended in collagen for 3D invasion individually and collectively. (b) Schematic of the dsDNA probe's binding scheme for dynamic single-cell gene expression analysis. (c) Multiphoton imaging of an invading cancer spheroid. Cells can invade individually as single detached cells and collectively as sprouts with leader-follower organization. Red, autofluorescence; white, collagen via second harmonic generation; green, Notch1 mRNA via dsDNA probe. Scale bar, 50  $\mu$ m.

at the leading edge of the sprout tip but also for monitoring of follower cells and detached cells.

## MATERIALS AND METHODS

**dsDNA Probe Design and Preparation.** The dsDNA probe consists of two oligonucleotide strands with alternating DNA and LNA monomers (Figure 1b). One strand, the donor strand, is 20 nucleotides long and designed complementary to the target RNA of interest. 6-FAM, the fluorophore used for fluorescence detection, is located at the 5' end of the donor strand. The second strand, the quencher strand, is 10 nucleotides in length. Iowa Black FQ, a dark quencher, is located at the 3' end of the quenching strand immediately adjacent to the fluorophore on the donor strand.

dsDNA probes were developed for the spatiotemporal gene monitoring of multiple mRNAs (Table S1). A random, scrambled probe with no known intracellular targets was developed as a negative control. The sequences of all dsDNA probes were verified through the NCBI Basic Local Alignment Search Tool for nucleotides (BLASTn). Transfection was performed by dissolving the donor and quencher strands in 10 mM Tris-EDTA buffer and 0.2 M NaCl before mixing them at a 1:2 molar ratio (donor/quencher). Finally, the probes were heated at 95 °C for 5 min in a dry block heater before cooling to room temperature gradually over the course of the next two and a half hours.

**Cell Culture and dsDNA Probe Transfection.** MDA-MB-231 mesenchymal triple negative breast cancer cells were cultured in DMEM (Corning, Manassas, VA) supplemented with 10% fetal bovine serum (Corning, Manassas, VA), 1% L-glutamine (Sigma-Aldrich, St. Louis, MO), and 0.1% gentamicin (Sigma-Aldrich, St. Louis, MO) at 37 °C and 5% CO<sub>2</sub> in a tissue culture incubator. For the transfection the cells were first plated in a 6-well plate at sufficient density to reach 90–95% confluence in 24 h. Then, the probe and Lipofectamine 2000 transfection reagent (Invitrogen, Carlsbad, CA) were combined according to the manufacturer's protocol prior

to transfection. In total, 3.33  $\mu$ g of probe was transfected per well, with 10  $\mu$ L of Lipofectamine 2000 transfection reagent used per well. The dsDNA probes targeting different genes were transfected in separate wells.

**Spheroid Formation and Culture in Collagen I.** Figure 1a illustrates the spheroid formation procedure. After a 12 h transfection (either through the day or overnight), the cells were harvested from the 6-well plate. Cells were washed twice with PBS, then exposed to 500  $\mu$ L of 0.25% trypsin-EDTA (Sigma-Aldrich, St. Louis, MO) for 2 min. After trypsin exposure, 1500  $\mu$ L of the DMEM culture media was added to each well and the cells were washed gently 10 times with a 1000  $\mu$ L pipet before addition to a 15 mL centrifuge tube to be spun down at 450 RCF for 5 min. After aspirating the trypsin and media, the cells were resuspended in enough culture media and methocel to create a mixture of 2000 cells per 20  $\mu$ L drop with 20% methocel per drop. The cell-methocel mixture was then placed on the underside of the lid of Petri dishes filled with 10 mL of 1× PBS. The cells aggregated into spheroids after 36 h of incubation at 37 °C and 5% CO<sub>2</sub> in a cell culture incubator. After spheroid formation, 200  $\mu$ L of spheroids were harvested by cutting the point off a 200  $\mu$ L pipet tip and added to 200  $\mu$ L of 3 mg/mL neutralized rat tail Collagen I (Corning, Corning, NY). The spheroid and Collagen I mixture were placed into a custom-made microscope viewing chamber that was 1.5 mm thick with a no. 0 coverslip attached for viewing.<sup>20</sup> The collagen-spheroid mixture hardened after 30 min in a cell culture incubator at 37 °C and 5% CO<sub>2</sub>. The viewing chamber was sealed with paraffin wax before imaging.

**Multiphoton Imaging.** A single-beam multiphoton microscope (TrimScope, LaVision BioTec, Bielefeld, Germany) was used for imaging (Figure 1c). The Chameleon Ultra2 titanium:sapphire laser used in the multiphoton imaging had a 120 fs pulse width at the sample (Coherent, U.K.). The samples were imaged using a long working distance water-immersion objective, with a 20 $\times$  magnification and 0.95 NA (Olympus, Center Valley, PA). The laser intensity at the

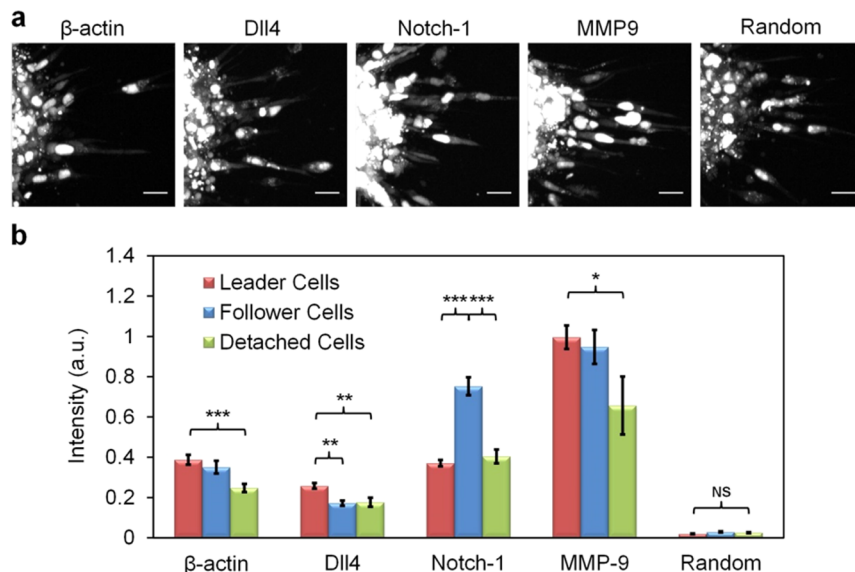


**Figure 2.** Gene expression profiling of invading cancer cells. (a) Fluorescence characterization of invading spheroids with dsLNA probes. Images are representative of at least five spheroids. Scale bars, 25  $\mu$ m. (b) Gene expression of invasive leader cells, follower cells (immediately following leaders), and detached cells was measured. Data are representative of four to five independent experiments ( $n = 160$  for  $\beta$ -actin,  $n = 131$  for Dll4,  $n = 160$  for MMP-9,  $n = 157$  for Notch-1,  $n = 156$  for random). \*\*\*,  $P < 0.001$ ; \*\*,  $P < 0.01$ ; \*,  $P < 0.05$ ; NS,  $P > 0.05$ .

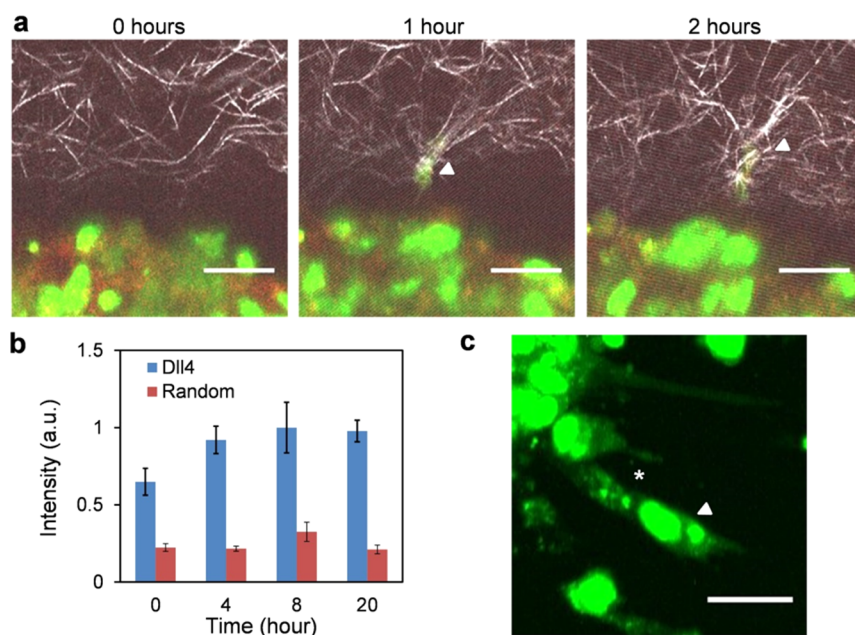


**Figure 3.** Dynamic analysis of collective cancer invasion. (a) Time-lapse multiphoton images of an invading sprout. The Dll4-expressing invasive leader cells (white arrow heads) sprout out from the cancer spheroid, deform the collagen fibers, and reorganize the extracellular matrix. Scale bars, 25  $\mu$ m; white, collagen; green, Dll4 mRNA. (b) Dynamic gene expression of Dll4 in invasive leader cells. The random probe is included as a control. (c) Dll4 expression seen in a multicellular sprout's leader (white arrowhead) is similar in the stalk cell (white asterisk) closer to the main spheroid. Scale bars, 25  $\mu$ m; white, collagen; green, Dll4 mRNA.

sample was adjusted for each imaging session by an electro-optical modulator (Conoptics, Danbury, CT) to ensure that the samples were always imaged with 120 mW of power. The samples were excited at 780 nm wavelength. Dichroic filters used included a 405 nm filter and a 490 nm filter. Band pass filters included 550/88 (fluorescein), 470/100 (autofluorescence), and 377/50 (second harmonic generation, for collagen I imaging). Three image channels were simultaneously detected through three photomultiplier tubes (two of the photomultiplier tubes were Gallium Arsenide, H7422A-40, Ham-

matsu, Hamamatsu City, Japan). To minimize photobleaching and acquisition time, images were taken every 2  $\mu$ m along the z-axis of the sample.

**Data Analysis and Statistics.** Data analysis was performed using NIH ImageJ software.<sup>21</sup> At least three samples were used per experiment unless otherwise stated. Data are shown as mean  $\pm$  SEM. Independent group comparisons were performed using the student's *t* test, and the comparison of multiple groups utilized a one-way ANOVA analysis with post hoc

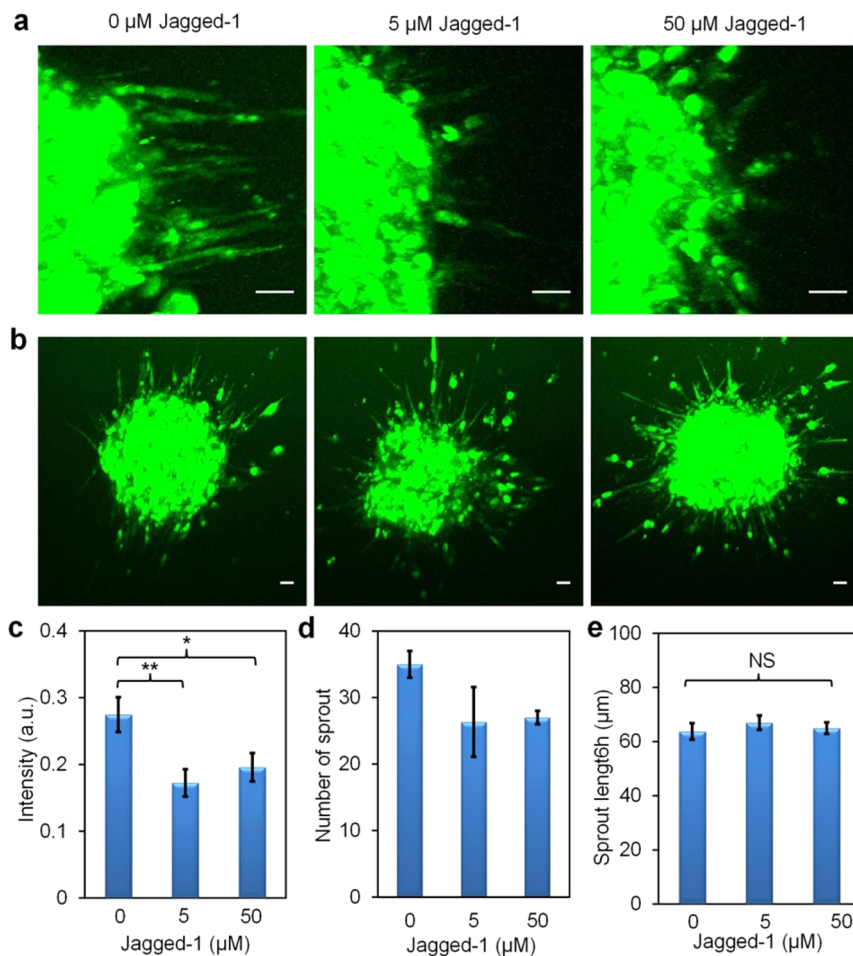


**Figure 4.** Jagged-1 increases Dll4 expression and enhances the formation of invading sprouts. (a,b) Maximum intensity projection of multiphoton images characterizing the invading spheroids treated with Jagged-1. Scale bars, 50  $\mu$ m. (c) Quantification of Dll4 mRNA in invasive leader cells with Jagged-1 treatment. (d) The number of spheroid sprouts with Jagged-1 with treatment. (e) The sprout length with Jagged-1. Data are representative from at least 3 spheroids for each concentration (\*\*\*,  $P < 0.001$ ; \*\*,  $P < 0.01$ ; \*,  $P < 0.05$ ).

Tukey's multiple comparison test.  $P < 0.05$  was accepted as statistically significant.

## RESULTS

**Notch-1 mRNA Expression Is Downregulated in Invasive Leader Cells But Not Follower Cells.** The dsDNA probes were transiently transfected into cancer cells for detecting collective cancer invasion of 3D spheroids. The fluorescence of the invasive cells as well as the detached cells and follower cells was observed and recorded (Figure 2). The probe sequence did not have a strong effect on the number of sprouts (Figure S1). Overall, MMP-9, a collagenase, and  $\beta$ -actin were upregulated in the invading sprouts, including leader and follower cells, compared to detached cells. In contrast, the random scrambled probe signal was not significantly changed in all cell types. Interestingly, we observed significantly increased Notch-1 expression in follower cells and increased Dll4 expression in invasive leader cells. These results indicate highly distinct gene expression profiles for different cells during collective cancer invasion. Importantly, differential expression of Dll4 and Notch-1 were observed in invasive leader cells and followers cells, suggesting Notch signaling may regulate 3D collective cancer invasion.

**Dll4 mRNA Is Increased during Initiating Tumor Sprout Leader Cells.** We investigated the dynamics of Dll4

in the invading sprouts. The dsDNA probe, along with time-lapse microscopy using a multiphoton microscope, enables us to simultaneously track the dynamic sprouting process in 3D cancer invasion as well as monitor the spatiotemporal gene expression distribution in invading sprouts (Figure 3). The surrounding collagen matrix can be monitored with the help of multiphoton imaging as second harmonic generation via a nonlinear scattering process, highlighting collagen I fibers without the need for fluorescence labeling. Using this technology, dynamic Dll4 cell expression was imaged in sprouts as they invaded the surrounding collagen I matrix (Figure 3a). Initially, no sprouts were seen at the collagen/spheroid interface; however, after 1 h of sprouting the cells could be observed extending into the surrounding collagen and deforming the collagen fibers toward the spheroid. At 2 h, the invading sprout could be seen invading farther into the surrounding collagen I, having sliced the initial collagen fibers to create a space to move. Additionally, the expression of Dll4 in invasive leader cell cytoplasms over time via dsDNA probe fluorescence is seen in Figure 3b. Over the course of 8 h of sprouting, the Dll4 signal increases by 35% before leveling off. For comparison, the random, scrambled dsDNA probe did not change significantly over the 20-h experiment.

Exogenous Jagged-1 decreases Dll4 expression and formation of invasive leader cells. Our results suggest the involvement of

Notch signaling in 3D collective cancer invasion. Therefore, a Notch ligand, Jagged-1, was used to modulate the Notch activity in sprouting spheroids (Figure 4a,b). We added Jagged-1, which decreased the Dll4 signal in invasive leader cells (Figure 4c). The number of sprouts per spheroid also decreased with Jagged-1 in a dose dependent manner (Figure 4d). In addition, Jagged-1 did not have an effect on the length of spheroid sprouts (Figure 4e). These results suggest Notch signaling may play an important role in 3D collective cancer invasion.

## ■ DISCUSSION

In this study, a dsDNA probe capable of probing dynamic single-cell mRNA gene expression during 3D collective cancer invasion was presented. By combining a 3D cancer invasion assay along with multiphoton imaging, our results highlighted not only the dynamics of multicellular signaling but also cell-matrix mechanical interactions during 3D collective cancer invasion. In particular, the dsDNA probe revealed a spatially differential expression pattern of genes involved in 3D cancer invasion, including not only leader and follower cells but also detached amoeboid-like cells as well (Figure S2). Consistent with the invasive nature of MD-MBA-231 cells, MMP-9 and  $\beta$ -actin upregulated in the invading sprouts. Phenotypically, the invasive sprouts of the spheroids appear to actively pull and lyse collagen I. These results suggest distinctive mechanisms may be involved in collective and individual invasion in 3D microenvironments. Further investigation is required to elucidate the mechanisms that regulate collective and individual invasion processes.

Our results also suggest the involvement of Notch signaling in 3D collective cancer invasion. Differential expression of Notch1 and Dll4 were observed in follower cells and leader cells. A Notch ligand, Jagged-1, is also shown to reduce the Dll4 mRNA expression in a dose-dependent fashion in invasive leader cells, suggesting an inhibitory role of Notch signaling in invasive leader cell formation. The above observations, along with Notch-1's decreased signal in invasive leader cells, highlight the spatial coordination of leader and follower cells during 3D cancer invasion, and the results are consistent with the suggestion that Notch-1 acts as a tumor suppressor.<sup>22</sup>

## ■ CONCLUSION

This study shows the applicability of the dsDNA probe as a flexible tool to monitor the real-time dynamics of mRNA expression during collective cancer invasion in 3D cell culture models. The mRNA distribution observed in invading sprouts suggests that cells at the edge of an invading sprout may be influenced by multiple biophysical and biochemical pathways. The capability of the dsDNA probe to elucidate contrasting gene expression in 3D culture assays carries important implications for the field as it not only improves the efficiency and speed in testing cancer chemotherapy drugs, but it also carries the potential to identify novel targets for antimetastasis therapy as well.

## ■ ASSOCIATED CONTENT

### Supporting Information

The Supporting Information is available free of charge on the ACS Publications website at DOI: [10.1021/acs.analchem.6b02608](https://doi.org/10.1021/acs.analchem.6b02608).

List of sequences for the dsDNA probe strands used in spheroids, effect of dsDNA probes on the number of sprouts, and detached cells display amoeboid-like phenotypes during collective cancer invasion ([PDF](#))

## ■ AUTHOR INFORMATION

### Corresponding Author

\*Phone: +1-814-863-5267. E-mail: pak@engr.psu.edu.

### Notes

The authors declare no competing financial interest.

## ■ ACKNOWLEDGMENTS

The authors thank Reza Riahi and Yuan Xiao for their valuable discussion and suggestions.

## ■ REFERENCES

- (1) Friedl, P.; Locker, J.; Sahai, E.; Segall, J. E. *Nat. Cell Biol.* **2012**, *14*, 777–783.
- (2) Cheung, K. J.; Ewald, A. J. *Oncotarget* **2014**, *5*, 1390–1391.
- (3) Cheung, K. J.; Gabrielson, E.; Werb, Z.; Ewald, A. J. *Cell* **2013**, *155*, 1639–1651.
- (4) Yamamoto, E.; Kohama, G.; Sunakawa, H.; Iwai, M.; Hiratsuka, H. *Cancer* **1983**, *51*, 2175–2180.
- (5) DiCostanzo, D.; Rosen, P. P.; Gareen, I.; Franklin, S.; Lesser, M. *Am. J. Surg. Pathol.* **1990**, *14*, 12–23.
- (6) Kats-Ugurlu, G.; Roodink, I.; de Weijert, M.; Tiemessen, D.; Maass, C.; Verrijp, K.; van der Laak, J.; de Waal, R.; Mulders, P.; Oosterwijk, E.; Leenders, W. *J. Pathol.* **2009**, *219*, 287–293.
- (7) Liu, L.; Duclos, G.; Sun, B.; Lee, J.; Wu, A.; Kam, Y.; Sontag, E. D.; Stone, H. A.; Sturm, J. C.; Gatenby, R. A.; Austin, R. H. *Proc. Natl. Acad. Sci. U. S. A.* **2013**, *110*, 1686–1691.
- (8) Gaggioli, C.; Hooper, S.; Hidalgo-Carcedo, C.; Grosse, R.; Marshall, J. F.; Harrington, K.; Sahai, E. *Nat. Cell Biol.* **2007**, *9*, 1392–1400.
- (9) Gaggioli, C. *Cell Adhesion & Migration* **2008**, *2*, 45–47.
- (10) Reffay, M.; Parrini, M. C.; Cochet-Escartin, O.; Ladoux, B.; Buguin, A.; Coscoy, S.; Amblard, F.; Camonis, J.; Silberzan, P. *Nat. Cell Biol.* **2014**, *16*, 217–223.
- (11) Riahi, R.; Sun, J.; Wang, S.; Long, M.; Zhang, D. D.; Wong, P. K. *Nat. Commun.* **2015**, *6*, 6556.
- (12) Tse, J. M.; Cheng, G.; Tyrrell, J. A.; Wilcox-Adelman, S. A.; Boucher, Y.; Jain, R. K.; Munn, L. L. *Proc. Natl. Acad. Sci. U. S. A.* **2012**, *109*, 911–916.
- (13) Riahi, R.; Dean, Z.; Wu, T.-H.; Teitell, M. a.; Chiou, P.-Y.; Zhang, D. D.; Wong, P. K. *Analyst* **2013**, *138*, 4777–4785.
- (14) Riahi, R.; Long, M.; Yang, Y.; Dean, Z.; Zhang, D. D.; Slepian, M. J.; Wong, P. K. *Integrative biology: quantitative biosciences from nano to macro* **2014**, *6*, 192–202.
- (15) Dean, Z. S.; Riahi, R.; Wong, P. K. *Biomaterials* **2015**, *37*, 156–163.
- (16) Gidwani, V.; Riahi, R.; Zhang, D. D.; Wong, P. K. *Analyst* **2009**, *134*, 1675–1681.
- (17) Hellstrom, M.; Phng, L. K.; Hofmann, J. J.; Wallgard, E.; Coultas, L.; Lindblom, P.; Alva, J.; Nilsson, A. K.; Karlsson, L.; Gaiano, N.; Yoon, K.; Rossant, J.; Iruela-Arispe, M. L.; Kalen, M.; Gerhardt, H.; Betsholtz, C. *Nature* **2007**, *445*, 776–780.
- (18) Dufraime, J.; Funahashi, Y.; Kitajewski, J. *Oncogene* **2008**, *27*, S132–S137.
- (19) Hoey, T.; Yen, W. C.; Axelrod, F.; Basi, J.; Donigian, L.; Dylla, S.; Fitch-Bruhns, M.; Lazetic, S.; Park, I. K.; Sato, A.; Satyal, S.; Wang, X.; Clarke, M. F.; Lewicki, J.; Gurney, A. *Cell stem cell* **2009**, *5*, 168–177.
- (20) Wolf, K.; Wu, Y. I.; Liu, Y.; Geiger, J.; Tam, E.; Overall, C.; Stack, M. S.; Friedl, P. *Nat. Cell Biol.* **2007**, *9*, 893–904.
- (21) Schneider, C. a.; Rasband, W. S.; Eliceiri, K. W. *Nat. Methods* **2012**, *9*, 671–675.

(22) Dai, Y.; Wilson, G.; Huang, B.; Peng, M.; Teng, G.; Zhang, D.; Zhang, R.; Ebert, M. P.; Chen, J.; Wong, B. C.; Chan, K. W.; George, J.; Qiao, L. *Cell Death Dis.* **2014**, *5*, e1170.